Biochemical Engineering Journal 135 (2018) 36–48

Contents lists available at ScienceDirect

Biochemical Engineering Journal

journal homepage: www.elsevier.com/locate/bej

Regular article

Technologies for large-scale umbilical cord-derived MSC expansion: Experimental performance and cost of goods analysis

Amanda Mizukami[a], Tania D. Pereira Chilima[b], Maristela D. Orellana[a], Mario Abreu Neto[a], Dimas T. Covas[a], Suzanne S. Farid[b,*], Kamilla Swiech[a,c,**]

[a] Hemotherapy Center of Ribeirao Preto, Faculty of Medicine of Ribeirao Preto, University of Sao Paulo, CEP 14051-140, Ribeirao Preto-SP, Brazil
[b] The Advanced Centre for Biochemical Engineering, Dept. of Biochemical Engineering, University College London, Gower Street, London WC1E 6BT, UK
[c] Dept. of Pharmaceutical Sciences, Faculty of Pharmaceutical Sciences of Ribeirao Preto, University of Sao Paulo, CEP 14040-903, Ribeirao Preto-SP, Brazil

ARTICLE INFO

Article history:
Received 4 July 2017
Received in revised form 16 February 2018
Accepted 25 February 2018
Available online 15 March 2018

Keywords:
Mesenchymal stromal/stem cells (MSC)
Cell expansion
Bioreactors
Bioprocess economics
Cost of goods (COG)
Reimbursement

ABSTRACT

The translation of cell therapies into clinical practice requires a scalable, efficient and cost-effective manufacturing process. This paper presents an integrated experimental and cost analysis of different cell culture technologies for umbilical cord-derived mesenchymal stromal/stem cell expansion: a multi-layer vessel (ML), a stirred tank bioreactor with microcarrriers (STR), a hollow fiber bioreactor (HF) and a packed-bed bioreactor (PB). The results showed that the cell proliferation rate, expansion fold and harvesting efficiency were highest in HF (36.8 ± 1.7 h; 9.8 ± 1.0 −fold; 100%). The STR, ML and PB achieved a similar level of cell number with high expansion folds (8.8 ± 0.39, 8.7 ± 0.90, 6.9 ± 1.3 −fold, respectively). However, harvesting efficiency was lowest with PB ($18\% \pm 0.77$), followed by STR ($61\% \pm 15.7$). The cells retained their functional properties post culture in all the technologies evaluated. The experimental results were incorporated into an advanced decisional tool comprising a bioprocess economics model and a stochastic model so as to evaluate the commercial economic feasibility and robustness of different candidate technologies for MSC manufacture. The model predicted that HF would be the least cost-effective option despite its advantageous experimental performance, due to its high consumable and equipment costs. ML ranked first in cost-effectiveness and robustness in this scenario followed by STR. The results also demonstrated how the bioprocess economics model can be used to direct improvements to the culture platforms so as to achieve commercial success according to the reimbursement level.

1. Introduction

Mesenchymal stromal/stem cell (MSC)-based therapies have increasingly gained importance over the years due to intense exploitation in basic studies and clinical trials for a broad range of diseases [1]. Numerous research groups have focused efforts on the large-scale expansion using different culture systems for achieving meaningful cell quantities for therapeutic purposes [2–7]. However, the establishment of a scalable, efficient, robust and cost-effective manufacturing process is still considered a challenge.

Different technologies for the expansion of MSC have already been described, with planar culture systems (2D), such as T-flasks and multi-layer vessels, the most used [8] due to their simplicity and satisfactory cell growth. Nevertheless, they are not sufficiently scalable when high cell demands are required [9–11]. More scalable systems need to be employed in order to make commercial scale expansion of MSC possible.

Bioreactor-based culture systems present major advantages over 2D culture and ensure the generation of high quality cell products, since these allow for full monitoring and control of all culture parameters, resulting in more precise and time-accurate interventions, while reducing the amount of manual operations required [2]. Various types of bioreactors have been employed for MSC expansion, such as stirred tank bioreactors with microcarriers [4,6], packed bed [5], rocking motion [7] and hollow fiber [3,12–15]. Each bioreactor has specific characteristics that should be evaluated in order to select the most appropriate one, considering the intended application. Moreover, to successfully meet the increasing demands, it is necessary to determine the operational and economic feasibility of each technology.

* Corresponding author.
** Corresponding author at: Hemotherapy Center of Ribeirao Preto, Faculty of Medicine of Ribeirao Preto, University of Sao Paulo, CEP 14051-140, Ribeirao Preto-SP, Brazil
E-mail addresses: s.farid@ucl.ac.uk (S.S. Farid), kamilla@fcfrp.usp.br (K. Swiech).

https://doi.org/10.1016/j.bej.2018.02.018

The use of advanced decisional tools has enabled the assessment of the financial feasibility of different processes, optimization, identification of process bottlenecks and suggestion of development targets required in order to achieve commercial success [16–18]. This approach has recently been extended to cell therapy bioprocessing [11,19–22].

Simaria and colleagues (2013) conducted a deterministic cost of goods (COG) analysis on the expansion process of MSC-based cell therapies identifying the most cost-effective technology to be used across different dose, demand and lot size scenarios. The group has identified the key cost drivers for the expansion of MSC as well as scenarios where the currently available technology fails to fulfill demand due to capacity constraints [11]. Furthermore, this analysis also identified the development effort required in order to allow current technologies to be able to meet future demands. Pereira Chilima and colleagues have taken this analysis further by modeling the whole production process and accounting for the process variability and operation features inherent to different technologies for adherent cell expansion [23].

This paper describes the expansion and functionality maintenance of MSC derived from umbilical cord matrix (UCM MSC) using different culture technologies (multi-layer vessel, stirred tank and hollow fiber bioreactors) and carried out a COG analysis in order to evaluate the economic feasibility of each one. A packed-bed bioreactor was also included in this study using data from our previous work [5] for comparative analysis. To the best of our knowledge, this is the first report comparing different technologies for a scalable *ex vivo* expansion of MSC. The COG analysis was conducted considering MSC application for the treatment of acute graft-versus-host disease (aGvHD), a possible serious complication of allogeneic hematopoietic cell transplantation (HCT). Since MSC have limited expansion potential [24–27], the process economics study first assessed the number of cell banks required by each technology evaluated and the associated costs. Following this, the manufacturing costs per dose for each process stage were calculated, and the deviations from these costs caused by technology-specific process variations were also taken into consideration. Furthermore, the key cost drivers for each process stage were identified and the COG as a percentage of sales was evaluated for each of the competing technologies across different reimbursement scenarios.

2. Material and methods

2.1. Mesenchymal stem/stromal cells (MSC)

MSC: were isolated from the umbilical cord matrix (UCM MSC) after informed approval and consent from the Institutional Ethical Review Board (Clinics Hospital, Ribeirão Preto Medical School, University of São Paulo, Protocol HCRP number 14906/2010). Briefly, a piece of umbilical cord (8 cm) was digested using 0.5% of collagenase type IA solution and incubated for 45 min at 37 °C. Afterwards the cell suspension was centrifuged at 250*g* and the cell pellet resuspended in Alpha Minimum Essential Medium (α-MEM) (Gibco, New York, USA) supplemented with 10% characterized fetal bovine serum (FBS) (HyClone, USA). The cells were then cultured on 75-cm^2 T-flasks at 37 °C and 5% CO_2 environment. The full mesenchymal cell isolation protocol from umbilical cords was described by de Lima Prata et al., 2012 [28]. Prior to inoculation into the cell culture technologies selected for this study, cells were grown on T-flasks (75/175 cm^2) at an initial cell density of 3,000 cells/cm^2 up to passage 4–5, using α-MEM containing 10% characterized FBS, 4.5 mM HEPES (Gibco, Burlington, Canada), 26.2 mM sodium bicarbonate (Merck, Darmstadt, Germany) and 1% penicillin/streptomycin (Gibco, Burlington, Canada). When 70% of confluence was achieved, cells were harvested using Tryple™ Express (Gibco, New York, USA) for 7 min at 37 °C. Cell number and viability were determined using the Trypan blue (0.4%) (Gibco, New York, USA) exclusion method. Different runs of monolayer expansion were performed to inoculate different runs of each technology.

2.2. Cell culture technologies

2.2.1. Multi-layer vessel

5,000 cells/cm^2 were inoculated (three different donors, n = 3) on 10-layer vessels (ML) (HyperFlask®, Corning, New York, USA) and grown at 37 °C under a 5% CO_2 humidified atmosphere. 50% of culture medium exchange was performed at day 3. After 6 days, cells were detached with Tryple™ Express (Gibco, New York, USA) and the cell number was quantified using Neubauer hemacytometer (Trypan blue exclusion method).

2.2.2. Stirred tank bioreactor

The Celligen® 310 (New Brunswick Scientific, New Jersey, USA) stirred tank bioreactor was used in this work. Since MSC are adherent cells, *Cultispher® S* microcarriers (Sigma Aldrich, Sant Louis, USA) (2.0 g/L) were used as anchoring support and prepared according to the manufacturer's instructions. UCM MSC previously expanded on T-flasks were inoculated in the STR containing microcarriers at 5,000 cells/cm^2 with a total cell culture medium volume of 800 mL (three different donors, n = 3). The adhesion phase comprised a stirring period (50 rpm for 1 min) followed by 30 min of no stirring. After 6 h of cell adhesion, a continuous stirring was set at 50 rpm. The cell culture parameters used were: pH 7.30, 20% of dissolved oxygen (DO) by headspace aeration (N_2, O_2 and air) and 37 °C (water jacket). The pH control at 7.30 was performed by adding base ($NaHCO_3$, 8%, Merck, Darmstadt, Germany) or acid (H_2SO_4, 2 M, Merck, Darmstadt, Germany). Samples of 5 mL were taken daily for cell quantification and metabolite analysis. Cell number was quantified using MTT enzymatic assay, as previously described [5]. From day 4 onwards, 50% of culture medium was changed every day. After 7 days of cultivation, all of the bioreactor content was transferred aseptically to a spinner flask for cell harvest. The cell culture medium was replaced by Tryple™ Express and stirred at 50 rpm for 20 min. The cell suspension was filtered using a 100 μm Cell Strainer (BD Biosciences) in order to remove the microcarriers and the recovered cells were quantified using Neubauer hemacytometer (Trypan blue exclusion method).

2.2.3. Hollow-fiber bioreactor

The Quantum Cell Expansion System® (Terumo BCT, Colorado, USA) was also employed in this work. Prior to cell inoculation (approximately 18 h), the hollow fibers were coated with human fibronectin (0.05 mg/mL, Corning, MA, USA) to promote cell adhesion. Thereafter, PBS was used to wash the system and culture medium (α-MEM + 10% FBS) was added. The culture medium was equilibrated with a gas mixture (5% O_2, 5% CO_2 and 90% N_2) to provide adequate aeration. Then, cells were inoculated (30×10^6 cells, 1,000 cells/cm^2) (two different donors, n = 2) in the intracapillary space (ICS) for cell adhesion (24 h). After this period, the cells were fed through a continuous flow of culture medium in the extracapillary space (ECS) at an initial rate of 0.1 mL/min with passive removal to waste. Sampling was performed daily in order to monitor glucose consumption and lactic acid production for cell growth estimation. As recommended by the manufacturer, the culture medium flow rate in the ICS was increased when the lactate concentration reached 8–9 mM and/or glucose concentration <5 mM. After 5 days of culture, cells were harvested with two cycles (180 mL each) of trypsin 0.5% (Gibco, New York, USA) treatment for 8 min. The recov-

ered cells were quantified by Neubauer hemacytometer (Trypan blue exclusion method).

2.2.4. Packed bed bioreactor

Previous published results from UCM MSC culture using a disposable packed bed bioreactor system (FibraStage®, New Brunswick Scientific) was used in this work for comparative analyses [5]. Briefly, 5,000 cells/cm^2 (passage 5) was inoculated in 10 g of immobilized carriers (Fibra-Cell disks) with 500 mL of culture medium and kept in incubator at 37 °C and 5% CO_2. 50% of media exchange was performed every day starting on day 5. Samples of Fibra-Cell disks and supernatant were taken every day and assessed for cell growth using MTT enzymatic assay and metabolism characterization, respectively. Cells were harvested from the scaffold after 7 days of culture using Tryple™ Express treatment for 30 min; being the number of cells quantified by Neubauer hemacytometer (Trypan blue exclusion method).

2.3. Cell characterization after expansion

After UCM MSC expansion in all culture technologies, the differentiation potential and immunophenotype profile were evaluated in order to verify the maintenance of functional characteristics. Immunolabeling was performed according to standard indirect immunocytochemistry protocols, using primary antibodies: CD13, CD14, CD29, CD31, CD34, CD44, CD45, CD49e, CD73, CD90, CD105 and Anti–HLA–DR (all from Becton Dickinson, San Jose, CA, USA). A minimum of 10,000 events were collected for each sample and the Cell-Quest™ software (Becton Dickinson, San Jose, CA) was used for acquisition and analysis [5]. Cells recovered from the technologies were induced to differentiation into adipocytes (α-MEM plus 15% FBS supplemented with 400 mL insulin, 100 mL indomethacin and 2 mL dexamethasone), chondrocytes (DMEM supplemented with 100 mM sodium pyruvate, 20% albumin, 20 mM ascorbic acid and 1 mM of dexamethasone) and osteocytes (α − MEM plus 7.5% FBS supplemented with 1 mL β-glycerol phosphate, 1 mL L-ascorbic acid and 2 mL dexamethasone) for 14, 15 and 28 days, respectively. The differentiated cells were stained with Sudan II-Scarlet for lipid droplets (adipocytes), von Kossa for mineralized bone matrix deposition (osteocytes) and Alcian Blue to assess proteoglycan synthesis (chondrocytes). All reagents were purchased from Sigma-Aldrich (Saint Louis, USA). The experimental procedure for differentiation potential and immunophenotype profile was described in detail in our previous work [5]. Metabolite analysis was performed with the culture medium supernatant collected throughout the cell culture period using a biochemical analyzer (YSI 2700, Yellow Springs Instruments, OH, USA).

2.4. Data presentation

Results of cell growth and cell characterization after expansion were presented as mean ± standard deviation (SD) (n = 3, three different donors for ML, STR and PB; n = 2, two different donors for HF). The harvesting efficiency (%) was determined based on the number of cells quantified in the sample measured before cell harvesting and the number of cells recovered at the end of harvesting procedure. Fold increase (FI) was calculated by the ratio of maximum cell number achieved (Nf) to initial cell number (Ni), ie, FI = Nf/Ni. The number of population doublings (PD) was calculated using the equation PD = log(FI)/log(2). Experimental results were compared using the nonparametric Mann-Whitney *U* test and considered statistical different when p-value <0.05.

2.5. COG analysis

2.5.1. Tool overview

The process economics tool described in Pereira Chilima et al. [23] was used in this study in order to evaluate the cost-effectiveness of different technologies for the manufacture of an UCM MSC-based therapy for the treatment of aGvHD.

Modifications to the tool were made in order to reflect the protocol used during practical experiments summarized in Sections 2.1–2.3. These modifications include performance parameters and protocols applied to the different technologies studied in this article such as: proliferation rate, the optimal cell culture period, harvesting efficiency and resource requirement. Microcarrier-specific parameters were also accounted for and adapted to the experimental protocol including: microcarrier selection (which dictates the surface area per gram of microcarrier) and the microcarrier seeding density. One important adjustment to the bioprocess economics tool was the addition of the PB bioreactor to the set of technologies included in the database. Another modification was the ability to compute the cell bank costs and the shipping costs. The experimental parameters used for the evaluation of the cell banking costs were: the initial cell number per umbilical cord (UC) donor, the number of expansion passages required for master cell bank (MCB) and working cell bank (WCB) production, the technology used for cell bank expansion and the proliferation rate of cells during cell bank formation. Fig. 1 (Supplementary section) summarizes the structure of the bioprocess economics tool, the experimental parameters included and how these integrate into the bioprocess economics tool.

2.5.2. Case study set up

The COG analysis focused on determining which cell culture technology would be the most cost-effective and robust for commercial scale production of an UCM MSC treatment for aGvHD. The clinical trial for this treatment is currently in phase I/II (process number: 404622/2012-7) and it is being conducted by the Hemotherapy Center of Ribeirão Preto (Ribeirão Preto Medical School, University of São Paulo). For early phase clinical manufacture, the cells have been expanded using T-flasks, washed and cryopreserved. The proliferation rate, harvesting efficiency and cell viability for alternative cell culture technologies were incorporated into the stochastic cost of goods model (see Tool Overview in the Section 2.5.1) to compute the cost benefits for each technology at commercial scale should this treatment be approved. Throught this case study, the different cost parameters included in the COG calculations of the different process steps have been described in Pereira Chilima [23].

Since MSCs have limited expansion potential, this study starts by identifying the number of cell banks required in order to satisfy the demand across the different technologies and the associated costs. Following this, the manufacturing costs per dose for each different process stage were calculated and the deviations from these costs caused by process variations characteristic of each different technology were also accounted for. Furthermore, the key cost drivers for each process stage were identified and the values of COG as% sales for each technology under different reimbursement scenarios was evaluated. COG as% sales is defined as the ratio of COG/dose to the selling price per dose.

2.5.2.1. Key assumptions.

2.5.2.1.1. Patient demand and dose. The cumulative dose size for the GvHD treatment described in this article is 4×10^6 cells/kg body weight. A maximum annual demand of 10,000 patients was assumed for this analysis based on the annual number of allogeneic bone marrow transplantation (BMT) (30,000) [29] and a rate of GvHD incidence of around 30% − 60% [30,31]. These patients

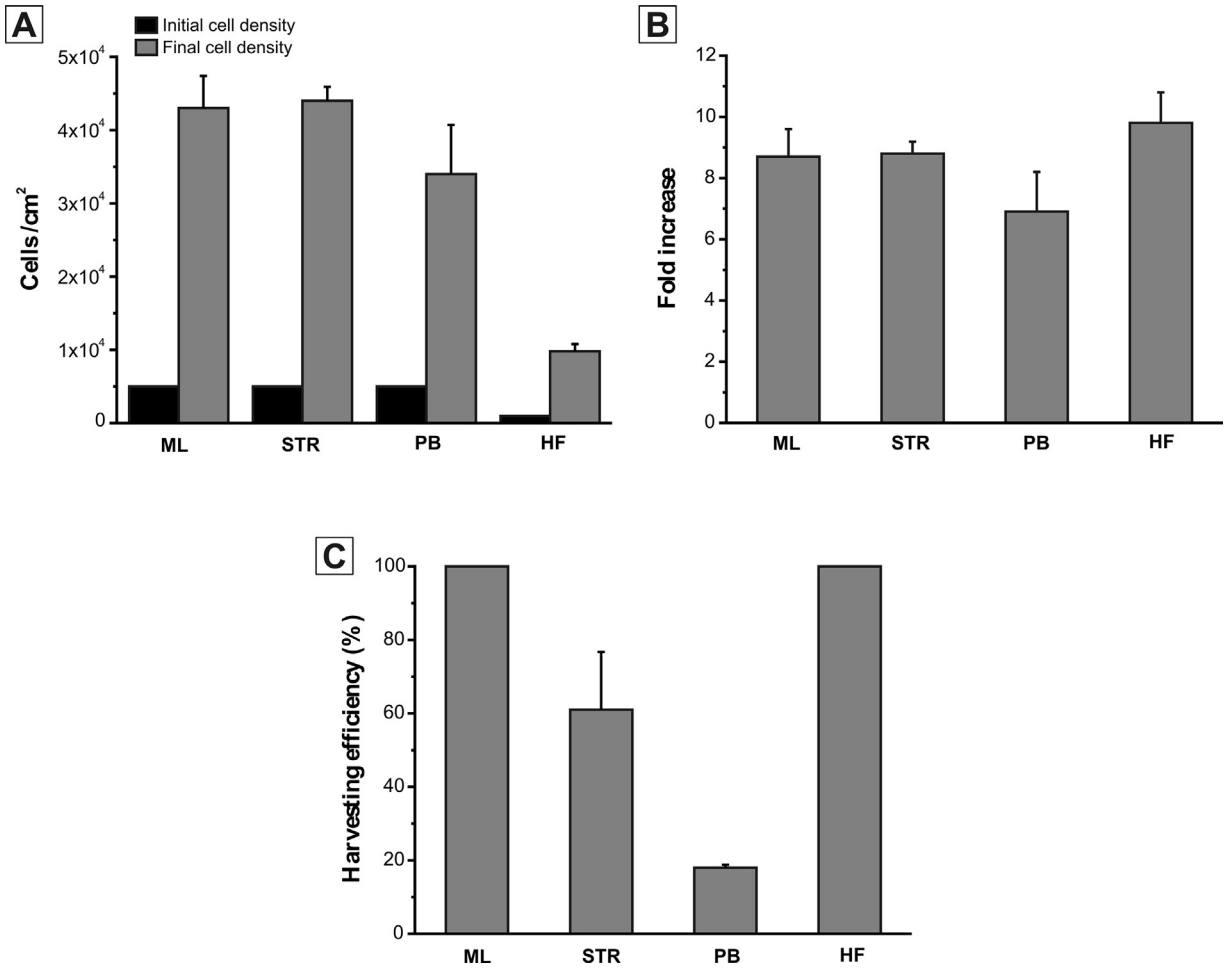

Fig. 1. UCM MSC expansion using different technologies. **(A)** Initial and final cell density. Culture time varied between the technologies in order to optimize cell harvesting: 6, 7, 7 and 5 days for ML, STR, PB and HF respectively; **(B)** Fold increase in cell expansion considering the amount of viable cells harvested per viable cells inoculated per cm^2; **(C)** Harvesting efficiency (%) at the end of culture was determined based on the number of cells quantified in the samples obtained before and after cell harvesting. Results are represented as mean ± SD (n = 3, three different donors for PB, STR and ML; n = 2, two different donors for HF technology). The results from PB bioreactor have been published previously and an authorization was obtained from the publisher to use some of data for comparative analysis [5].

would ideally be scattered across the globe and hence the average patient weight used was the world average person weight, ~69 kg. The minimum and maximum patient weights were also used in this analysis and were considered to be 60.7 kg (Africa) and 80.7 kg (North America) respectively [32].

2.5.2.1.2. Cell bank stage. The isolation of MSC from the umbilical cord yields between 1×10^6 to 5×10^6 cells per umbilical cord (UC), and therefore, this range was used to illustrate the variation in number of donors required yearly to fulfill a specified demand. A mean value of 3×10^6 for cells retrieved from a UC donor was selected. It was also assumed that 5×10^7 cells from each UC were used for testing after cell culture passage number 4. The bioprocess economics model assumed that during cell bank formation cells were cultured in tissue culture flasks (T175 cm^2) through 3 expansion passages forming a MCB. After this process, the cells are cryopreserved in vials and thawed when needed to produce a WCB. During the formation of the WCB a further two expansion passages were carried out before inoculation into a bioreactor (passage 5). For both MCB and WCB, each cell expansion lasted for 7 days with two intermediate media exchange steps. It was assumed that the maximum number of cell banks that a single team can process per year is 100, and hence scenarios where the number of cell banks required exceeds this limit were deemed infeasible.

By using the initial cell number isolated from the UC, the cell proliferation rate and the mean fold increase achieved during the cell expansion, it is possible to evaluate the number of cells banks required as follows:

$$NCB = D/(YDSPi \times (1\text{-}RBF) \times Y_{harvesti} \times R_{proliferationi} \times N_0 \times 2^{(Te \times ES/Td)}$$

Where D is the annual demand in doses per year, Y_{DSPi} and $Y_{harvesti}$ are the downstream process yield and the harvest yield of each technology i (Table 1). R_{BF} is the batch failure rate, $R_{proliferationi}$ is the proliferation rate of the cells in technology i given in fold increase over cell culture period, N_0 is the initial number of cells retrieved from the umbilical cord, ES is the cumulative number of expansion stages from MCB to WCB formation. Te and Td are both given in days, Te is the duration of each cell expansion stage and Td is the doubling time in technology i (Table 2).

All of the assumptions made in this case study regarding the cell banking stage are based on the experience of the cell banking team and the ongoing Phase I/II multi-clinic clinical trial for the treatment of aGVHD at the Hemotherapy Center of Ribeirão Preto (Ribeirão Preto Medical School, University of São Paulo).

2.5.2.1.3. Cell culture & DSP stage. In this case study, DSP involves a wash and concentration step with a kSep centrifuge and for the STR there is also a microcarrier removal stage prior to this. The decisional tool described in Pereira Chilima et al. [23] was slightly modified and adapted to the results attained from the experiments described in Section 2.2, since each technology has a different cell culture time, harvesting efficiency and proliferation

Table 1
Key technology specific assumptions used in and produced by the process economics tool.

Process stage	Parameter name	Value				Unit
Cell expansion	Technology name	ML-36	STR 500	PB 500	HF	–
	Cell culture vessel working volume	24	250	42	4.2	L/unit
	Surface area	122,400	3,750,000	500,000	21,000	cm^2/unit
	Culture medium volume	0.2	0.05	0.083	0.2	mL/cm^2
	Nr of bioreactors/tissue culture flasks used	55	1	15	207	–
	Incubator capacity	12	–	–	–	Bioreactors/tissue culture flask/unit
	Cell culture length	6	7	7	5	Days
	Start culture duration	1.3	3	1	0.17	h/unit
	Medium exchange duration	0.67	1.5	0.5	0	h/unit
	Harvest duration	0.67	1.5	0.5	0.2	h/unit
	Number of executing operators required	6	3	3	26	Operators
	Number of documentation operators	6	2	2	13	Operators
	Consumable costs	5.8×10^{-2}	0.19×10^{-2}	5.6×10^{-2}	57.14×10^{-2}	USD/cm^2
	Incubator costs	17,835	–	–	–	USD/unit
	Skid costs	–	198,847	300,000	150,000	USD/unit
DSP	DSP yield	68	61.2	68	68	%
	Total DSP time	1.15	3.67	1.26	2.23	h

ML: compact multi-layer (e.g. Hyperstack®, Corning), STR: stirred tank bioreactors with microcarriers (e.g. BIOSTAT®, Sartorius, PB: packed bed (e.g. iCellis®, Pall Life sciences), HF: hollow fiber bioreactors (e.g. Quantum®, Terumo BCT). A maximum time for DSP to be carried out was set to 4 hours, the differences in time seen are attributed to the difference in the volume loaded into the kSep system. In this case, it was assumed that for each cell culture vessel the volume loaded into the kSep would be equal to 1/3 of the medium volume in the bioreactor at the last expansion stage. For microcarrier-based cell culture, the time taken to remove the microcarriers from solution was also accounted for. The costs are expressed in USD (US dollars). The process economics tool used to compute labor requirement and DSP time is described in detail in Pereira Chilima et al. [23].

rate. Fig. 1 (Supplementary section) shows the key inputs and outputs of this modified decisional tool. Table 1 highlights some of the key assumptions for the different stages in terms of mass balancing, sizing and resource requirements. Key differences between the cell culture technologies can be seen in the media requirement, surface area per unit and labor requirement. The labour requirement for each technology was evaluated considering the number of manipulations required. The ratio between the executing operator and the documenting operator was set to 1:1 for the manual multi-layer flasks, and 2:1 for the remaining automated technologies.

2.5.2.1.4. Shipping costs. The only costs considered at this stage were the labor costs and transportation costs. The labor costs were calculated using a case study by Lowdell [33], which described a scenario where 3 FTEs were required to fill enough dry shippers for 10,000 doses per year. The transportation costs were attained through an interview with an experienced courier of cryogenic materials. They identified that the cost of transportation per shipment of cryogenic material across continents is between USD 2.6–4.1 k; the value chosen in this analysis was the average, USD 3.3 k. These costs include the coordination with the destination of choice, adequate documentation, equipment, coordination with the airport security system in order to avoid submitting the product to x-ray scans and door-to-door hand carry.

3. Results and discussion

3.1. UCM MSC can be efficiently expanded using different scalable technologies

Two different types of bioreactors (STR and HF) and a multi-layer vessel (ML) (10-layer flask) were evaluated regarding expansion and harvesting efficiency of UCM MSC. To extend this study, we compared the technologies here evaluated with the PB, used for UCM MSC expansion in our previous work [5]. Although limited in scalability, ML was considered in this study due to its simplicity and widespread use by cell therapy companies engaged in MSC-based clinical trials [34].

Figs. 1A and B show the initial and final cell density (cells/cm^2), as well as the expansion fold-increase obtained using the different technologies. The ML and HF do not allow daily cell sampling and hence it is not possible to obtain the cell growth profile during cultivation. The duration of the cultures varied according to the culture technology used. The rationale was to extend the culture time as long as possible to maximize cell expansion whilst avoiding overconfluence and cell-cell/cell-matrix clustering, which could prevent an efficient cell harvesting. As can be seen in Fig. 1A, with the same initial cell density (5,000 cells/cm^2) a similar level of cell expansion was observed for the STR and ML, achieving $4.4(\pm0.19) \times 10^4$ and $4.3(\pm0.44) \times 10^4$ cells/cm^2, respectively. A slightly lower amount of cells was obtained in the PB bioreactor ($3.4\ (\pm0.67) \times 10^4$ cells/cm^2). In the HF, a total cell density of $9.8(\pm1.01) \times 10^3$ cells/cm^2 was obtained, using five times less initial cell density (1,000 cells/cm^2) compared to the other technologies. Experiments using higher seeding densities were performed in HF, however, due to harvesting difficulties (formation of cell aggregates), the number of cells recovered were lower than obtained using 1,000 cells/cm^2 (data not shown). Despite the lower final cell density, HF presented the highest fold-increase (9.8 ± 1.0) in 5 days, followed by STR, ML and PB at day 7, 6 and 7 (8.8 ± 0.39, 8.7 ± 0.90, 6.9 ± 1.3, respectively) (Fig. 1B).

Doubling time is another important parameter that acts as an indicator of the cell adaption in the culture technology. An average doubling time (total doublings divided by culture time) was calculated for each technology. According to the fold-increase results, the shortest doubling time of UCM MSC was observed in the HF (36.8 ± 1.7 h), followed by ML, STR and PB (Table 3).

Regarding cell metabolism, the feeding regimen adopted in the ML (50% of culture medium exchange at day 3), PB (50% of culture medium replaced every day after day 5), STR (50% of culture medium replaced every day after day 4), HF (perfusion) avoided glucose and glutamine exhaustion. As a result of glucose and glutamine consumption, lactate and ammonia were produced. Nevertheless, the maximum concentrations achieved in the experiments never reached inhibitory levels for MSC growth (35 mM and 4 mM for lactate and ammonia, respectively) [35].

In contrast with recombinant protein production processes in which the protein is the product and hence cell damage during harvesting is not a problem, in the MSC-based therapy, cells are

Table 2
Key general assumptions used in and produced by the process economics tool.

Process stage	Parameter name	Value	Unit
General	Patient weight	Tr(60.7,69,80.7)	kg/patient
	Demand	10,000	Patients per year
	Nr lots	100	Lots per year
	Depreciation period	8	Years
	Lang factor	23.67	–
	Shift time	8	h/shift
	Clean room time	6.4	h/shift
	Batch failure rate	Tr(0,5.10)	%
	Line management ratio	1.5	–
	Operator QMS ratio	1.3	–
	Culture medium	450	USD/L
	Tryple & Trypsin	98	USD/L
	Operator salary	120,000	USD/operator per year
Cell bank	Cells retrieved per umbilical cord	$Tr(1 \times 10^6, 3 \times 10^6, 5 \times 10^6)$	–
	Cells doubling time	36	h
	Number of expansion passages for MCB formation	3	Expansion passages
	Number of expansion passages for WCB formation	2	Expansion passages
	Cell culture vessel(s) used	1-layer cell culture flask (ML1),2-layer cell culture flask (ML2),40-layer cell culture flask (ML-40)	
	Number of cell culture vessels used	1 (ML1), 1(ML2), 47 (ML40)	Units per cell bank
	Medium consumption	0.25 (ML1 & ML2), 0.16 (ML40)	mL/cm^2
	Number of skids required (ML40 only)	3	Units
	Number of incubators required	3	Units
	Number of executing operators required	4	Operators
	Executing operator: documenting operator ratio	2	–
	Cells retrieved for testing	5×10^7	Cells per cell bank
	Final number of cells attained per cell bank (Post WCB formation) (mean,SD)	$5.04 \times 10^{10}, 1.06 \times 10^{10}$	Cells per cell bank
	Cell culture vessel cost	USD 60(ML1), USD 73(ML2), USD 1265 (ML40)	USD/unit
	Skid cost (ML40 only)	USD 425,000	USD/unit
	Incubator cost	USD 30,000	USD/unit
	QC cost/MCB	USD 75,000	USD/MCB
Cell expansion	Microcarrier used	*Cultispher® S*	–
	Microcarrier seeding density	2	g/L
	Bioreactor space efficiency (STR)	50	%
	Microcarrier cost	5	USD/g
	QC cost	USD 3,333	USD/lot
DSP	Technology used	kSep400®	–
	Number of units used	1	–
	Number of chambers used	4	–
	Number of cycles used	1	–
	QC cost	USD 6,666	USD/lot
Shipping	Number of operators required	3	Operators/year
	Vials/shipment	50	–
	Cells/vial	60 M	cells/vial
	Transportation cost per shipment	USD 3,774	USD

Clean room time was calculated under the assumption that operators would spend 80% of a shift in the clean room and the remaining 20% were of this time was spent gowning and degowning and carrying out documentation. The total QC costs (DSP + Cell expansion) was assumed to be USD 10000. This value was evenly divided between: Cell expansion, Cell wash & concentration and filling. Hence 1/3 of these costs were attributed to cell expansion and the remaining 2/3 to DSP (cell wash & concentration and filling). The cell factory bioreactors modeled (CS1, CS2, CS40) correspond to the Nunc cell factory systems. Since the focus of this paper is on the upstream technologies, additional data on the DSP cost components considered in this article can be found on Hassan et al. [19]. The costs are expressed in USD (US dollars). The process economics tool used to carry out the mass balance for the cell banking stage is described in detail in Pereira Chilima et al. [23].

Table 3
Culture parameters for the expansion of UCM MSC in the different technologies tested. Results are represented as mean ± SD (n = 3, three different donors for PB, STR and ML; n = 2, two different donors for HF technology).

Technology	Average doubling time (hours) (±SD)	Population Doublings (PD)	Initial cell density ($cells/cm^2$)	Harvested cells ($cells/cm^2$) (±SD)	Culture duration (days)
ML	47 ± 2.3	3.1 ± 0.2	5,000	$4.3 \times 10^4 \pm 4.4 \times 10^3$	6
STR	54 ± 1.1	3.1 ± 0.06	5,000	$2.7 \times 10^4 \pm 7.9 \times 10^3$	7
PB	61 ± 6.3	2.8 ± 0.3	5,000	$6.1 \times 10^3 \pm 1.2 \times 10^3$	7
HF	37 ± 1.7	3.3 ± 0.1	1,000	$9.8 \times 10^3 \pm 1.0 \times 10^3$	5

the final therapeutic product. For this reason, the *ex vivo* expanded cells need to be efficiently harvested from the culture system, while maintaining their functional characteristics and therapeutic potential. In addition, it is necessary to consider the harvesting strategies especially when developing large-scale expansion to ensure a feasible bioprocess [36]. Taking this into consideration, the harvesting efficiency was evaluated in the different technologies used (Fig. 1C). In all the experiments presented herein, the harvesting efficiency (%) was determined based on the number of cells quantified before cell harvesting and the number of cells recovered at the end of harvesting procedure. The cells harvested in the STR and PB, unlike ML and HF (Trypan blue exclusion method), were quantified using an enzymatic method (MTT assay) due to the difficulty of achieving efficient cell retrieval from the scaffold, thus avoiding the

underestimation of the amount of cells. Thus, it is important to emphasize that the harvesting efficiency of the technologies was compared under these differences in the quantification methods. A low harvesting efficiency was attained in the PB (18% (±0.8)), due to insufficient time of enzyme treatment and to gentle platform motion, which prevents efficient enzyme diffusion throughout the bed, even when testing other conditions [5].

The STR presented a harvesting efficiency of 61% (±15.7). Cell harvesting from microcarriers is challenging due to intense cell-cell/cell-matrix agglomerates formation and microcarrier bridging during cultivation and different patterns of cell adhesion, which depend on the microcarrier characteristics (charge, porosity, surface) and culture conditions. This situation has been described previously in literature [37–40]. Despite the intense cell-microcarrier agglomeration observed, the harvesting efficiency obtained in this work (61% ± 15.7) is similar to other studies reporting MSC small-scale expansion on microcarriers (70–95% of cell harvesting) [38–41]. It is worth mentioning that the majority of studies on large scale MSC bioreactor-based expansion do not mention the harvesting efficiency (%) [6,10]. In a recent paper, Nienow et al. [36] reported an efficient method for cell harvesting using intense agitation and a suitable enzyme solution (0.25% (v/v) trypsin and 0.02% (w/v) EDTA), achieving an overall harvesting efficiency of more than 95%. Despite the satisfactory level of expansion in STR, the cell harvesting stage should be extensively studied and improved for each microcarrier type to allow commercial exploitation of MSC cultured in this technology.

In the HF, a harvesting efficiency of 100% was assumed based on manufacturer (Terumo BCT) experience and since two cycles of trypsinization were performed, with no significant increase in cell number in the last one (cell counting using Trypan blue exclusion method), inferring that all cells were successfully retrieved. Since daily cell quantification and confluence status is not possible in this bioreactor, a static control (T-flask) with the same initial cell density was performed in parallel to infer the cell growth. Then, when the static control achieved 80–90% of cell confluence, the experiment in the HF was ended. This strategy was efficient to avoid overconfluence and to release cells without clustering. In the ML vessel, the same assumption was made. After 80–90% of confluence (6 days), the cells were trypsinized and quantified. A visual observation in the optical microscope was performed after the harvesting step, indicating that no cells remained attached on the static control vessel (100% of harvesting efficiency).

Among all the technologies tested, the STR is the most common technology used in the biopharmaceutical industry and is responsible for the majority of FDA-approved biopharmaceuticals [43]. For this reason, the gained experience facilitated the transition to stem cell bioprocessing and many reports for MSC expansion in an STR bioreactor have been described. Rafiq and colleagues [6] cultivated MSC from bone-marrow (BM-MSC) in a fully controllable 5L STR with non-porous microcarriers plastic P-102L and were able to produce a maximum cell density of 1.7×10^5 cell/mL, achieving a fold-increase of >6. Similarly, Jing et al. [10] evaluated the BM-MSC expansion in a single-use STR (Mobius CellReady 3-L) and achieved 2.0×10^5 cell/mL after 12 days. Hupfeld et al. [44] reported the expansion of MSC from umbilical cord matrix in a 1.5L controlled stirred tank bioreactor using Cytodex-1 microcarrier. However, the authors did not clearly state the maximum cell number obtained in the stirred system. In the present work, higher cell concentrations (maximum of 6.6×10^5 cell/mL at day 7) were obtained when compared with the reports previously cited, even when considering the moderate harvesting efficiency obtained (approximately 4×10^5 cell/mL).

The HF, a fully-closed technology, has advantages related to automation and reduction of labor-intensive tasks, making it appropriate for bioprocesses and in accordance with GMP guidelines [12]. The total cell number achieved in our study ($2–3 \times 10^8$ cells) was similar to that obtained in previous reports using the same HF (Quantum Cell Expansion System®) [3,14,15]. However, our study shows the production of a large number of cells in a short period of time (5 days), potentially representing cost and time savings.

Although many studies are focused on fully scalable, automated and GMP-compliant technologies for MSC expansion, planar flask cultures and multi-layer vessels are commonly used to produce high amounts of MSC. According to Schirmaier et al. [45], a range of $2.5 \times 10^8–1 \times 10^9$ cells can be achieved using 10–40 layer CellSTACKs® (Corning, New York). However, the maintenance of cell quality, process monitoring and scalability are difficult to ensure. Moreover, the lack of control of culture parameters in planar cultures (pH, dissolved oxygen, temperature) could affect the consistency and safety of the cell product [2]. It is worth mentioning that cell growth can be monitored in these cultures through the analysis of the consumption of substrates (glucose and glutamine) and formation of by-products (lactate and ammonia).

For the successful implementation of a culture technology for MSC expansion, several important parameters need to be assessed. These include cell production per growth area, harvesting efficiency and maintenance of functional characteristics post-culture. In the present work, it was possible to perform an efficient UCM MSC expansion in the different technologies evaluated, however some improvements could still be performed, particularly in order to increase the cell harvesting in STR and PB. The lack of in-depth optimization could be the responsible for the differences of performance between the technologies and the available data from the literature. The bioprocess optimization could not only maximize cell production, harvesting efficiency and reproducibility at some degree, but also change the technologies ranking for scalability, robustness and even cost-effectiveness.

The experimental research here presented suggested that HF would be more suitable for large-scale production of MSC (cost analysis not yet considered), due to the highest fold-increase in a short period of time and highest harvesting efficiency. Moreover, the combination of single-use and closed technology are desirable features of the HF for GMP commercial MSC manufacturing. STR and PB also presented promising results in terms of cell production, but the harvesting efficiency was challenging and further studies need to be performed to optimize this parameter.

3.2. UCM MSC retain functionality after expansion

After expansion, in order to ensure the UCM MSC functionality, the differentiation potential and immunophenotype profile by flow cytometry were evaluated in all technologies tested. The cells demonstrated trilineage differentiation potential into adipogenic, chondrogenic and osteogenic cells, as established by the International Society for Cellular Therapy (ISCT) (Fig. 2). Fat droplets (adipocytes) became apparent after 14 days of induction (Sudan-II Scarlate staining) (Fig. 2A); calcium deposit after Von Kossa staining confirmed the differentiation into osteocytes at day 28 (Fig. 2B). Proteoglycan formation (chondrocytes) was also observed, confirmed after Alcian blue staining (Fig. 2C). Fig. 2 (Supplementary section) presents the differentiation images obtained for all culture technologies.

Regarding immunophenotype profile, no significant differences ($p > 0.05$) in the levels of expression of surface antigen markers were observed before and after cell culture in all the technologies. Fig. 2D shows that the expression of CD73 and CD90 presented positivity ≥92% and negative expression (≤2.5%) for CD14, CD45, CD34, HLA-DR for ML, STR, PB and HF (post expansion). According to the ISCT criteria, MSC must present expression >95% for CD73, CD90

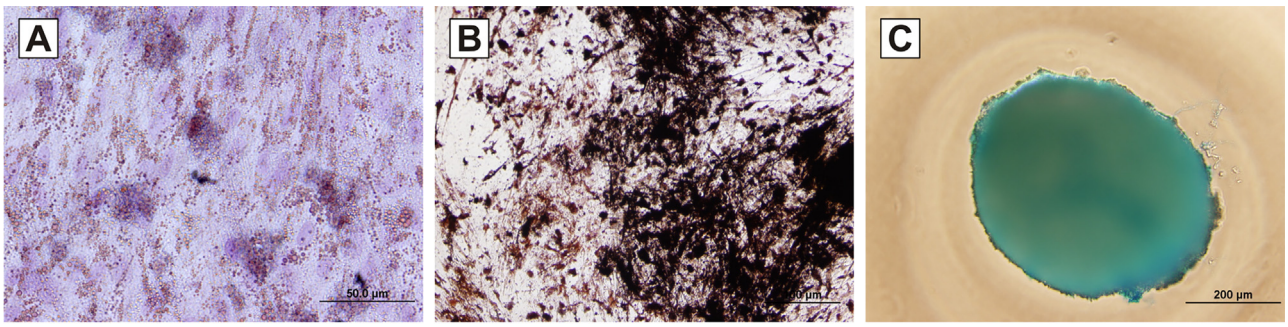

D

	ML vessel				STR bioreactor				PB bioreactor				HF bioreactor			
	Pre-expansion		Post-expansion		Pre-expansion		Post-expansion		Pre-expansion		Post-expansion		Pre-expansion		Post-expansion	
Cell surface markers	Mean	SD	Mean	SD	Mean	SD	Mean	SD	Mean	SD	Mean	SD	Mean	SD	Mean	SD
CD13	98.0	0.8	99.0	0.8	93.9	6.9	98.2	0.9	99.0	0.3	88.1	8.9	97.1	2.8	98.0	0.1
CD14	0.3	0.4	0.8	0.1	1.0	0.5	0.6	0.5	1.1	0.3	1.5	0.9	0.0	0.0	0.9	1.2
CD29	97.0	2.5	98.8	1.4	94.0	9.6	96.8	2.5	99.4	0.2	93.5	9.6	97.1	2.9	97.8	0.1
CD31	1.1	1.1	0.2	0.0	1.3	0.2	0.5	0.3	0.6	0.2	0.3	0.1	0.4	0.6	0.2	0.0
CD34	0.4	0.6	0.6	0.4	1.1	0.4	0.7	0.5	1.4	0.6	2.5	1.7	0.6	0.8	0.1	0.1
CD44	96.9	1.5	95.9	1.2	90.3	7.7	86.6	11.9	93.5	6.8	77.6	21.0	94.7	5.8	90.5	3.3
CD45	0.4	0.5	0.1	0.0	0.9	0.2	0.6	0.4	0.6	0.3	0.3	0.1	0.2	0.3	0.2	0.2
CD49e	98.5	0.3	97.8	1.2	93.1	8.2	90.4	7.0	97.4	1.6	84.8	14.4	97.1	2.6	93.5	0.9
CD73	95.5	2.4	94.7	0.4	91.9	5.4	92.0	7.0	91.0	8.7	81.0	17.9	89.5	3.9	92.6	1.5
CD90	99.2	0.5	99.3	0.5	96.1	5.7	96.2	4.4	99.5	0.3	95.7	3.6	98.3	1.9	98.5	0.6
CD105	95.4	2.4	96.6	0.8	90.5	9.6	74.1	12.1	85.7	15.3	50.2	13.3	92.6	7.2	87.8	0.3
HLA-DR	0.6	0.2	0.4	0.5	0.7	0.3	0.6	0.5	0.8	0.3	0.7	0.5	0.1	0.1	0	0

Fig. 2. Functional characterization of expanded UCM MSC. Multilineage differentiation ability was performed for all technologies; **(A)** adipocytes were evidenced after 15 days by discrete fat droplets formation (Sudan-II Scarlate staining), **(B)** osteocytes after mineralized calcium formation (von Kossa staining) and **(C)** chondrocytes by proteoglycan formation after 14 days (alcian blue staining)*; **(D)** Immunophenotypic expression of a specific surface antigen of UCM MSC before and after culture in the PB, STR, ML and HF technologies. Expression percentage of isotype control of all analyses performed was <1.5%. *The trilineage differentiation illustrated is representative of all technologies evaluated.

and CD105 and also expression <2% for CD14, CD45, CD34, HLA-DR [46]. The cell surface marker CD105 presented percentage <70% after culture in STR and PB, and a slightly lower percentage <90% for HF. Nonetheless, the differences observed before and after expansion were considered not statically significant ($p > 0.05$) due to large standard deviation observed (Fig. 2D). Expression percentage of isotype control of all analyses performed was <1.5%. The decreased CD105 expression observed for STR and PB post-culture may be attributed to the longer time of enzymatic cell detachment (20 min for STR and 30 min for PB) due to the difficulty in cell harvesting, which is known to affect surface receptors. This phenomenon has been reported previously [2,40,47]. Mendicino and coworkers (2014) performed a compilation of 66 Investigational New Drug (IND) submissions to the FDA for MSC-based products and found substantial variability in cell surface markers, especially for the CD 105 marker. These MSC-based IND found CD105 expression levels as low as 80%. The authors question whether the quantitative difference in expression level is really relevant for MSC characterization [48]. Although this is a concerning effect for MSC phenotype, we realized that this is only a transient effect since it was demonstrated that the loss of CD105 expression can be reverted upon few days of static culture [2]. In addition, the functional properties of the cells (differentiation – present study – and potential to inhibit the proliferation of T-lymphocytes *in vitro* – others studies conducted by the group) was not affected by the observed reduction in CD105 expression. Despite the ISCT requirements are followed by many researchers, the MSC minimal criteria have been revised over the years trying to improve some aspects like nomenclature, heterogeneity, markers.

It is important to mention that immunological assays (inhibition of T-lymphocyte proliferation and cytokine release assay) are recommended in the validation process and/or pre-clinical phase to assess the immunomodulatory properties of MSC produced [49] and would be required for future MSC application in the treatment of aGvHD.

3.3. COG analysis for the different expansion technologies

3.3.1. Cell bank cost analysis

One of the drawbacks of using MSC in large scale processes is the need of multiple cell banks per year, due to the limited expansion potential of these cells [24–27]. Fig. 3 shows the cell bank requirements and the associated costs across the technologies studied in this article. Fig. 3A shows that PB requires the highest number of UC donors and hence MCBs, due to the low level of cells recovered at the end of the culture (harvesting efficiency of 18%). PB is followed by the technology with the second lowest cell detachment yield, the STR with microcarriers. Moreover, PB is the only cell culture technology which may require a higher number of UC donors to produce 10,000 doses per year than those which a single team of operators can process within that period, with a 15% probability of surpassing this limit. Both, the HF and ML have a harvesting efficiency of 100% and therefore, require the lowest number of UC donors, highlighting the benefits of these technologies. The HF required the lowest number of MCBs since cells grow at a relatively high proliferation rate (low average doubling time). An additional advantage of HF is the requirement for low seeding densities compared to ML due to the relatively high proliferative rate (Table 3). Fig. 3B shows that

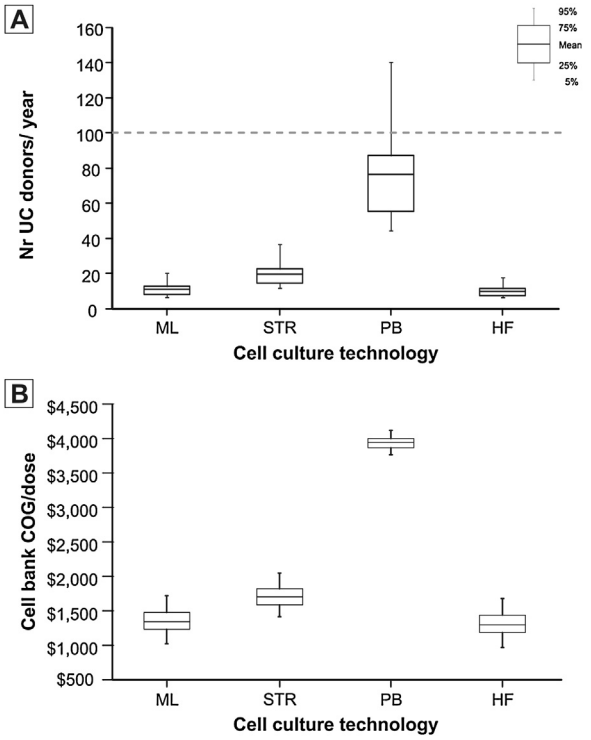

Fig. 3. **(A)** Distribution of number of donors required to manufacture 10,000 doses per year across multiple technologies. (**B)** Distribution of MCB and WCB costs per dose across multiple technologies for a demand of 10,000 patients per year. This distribution was achieved through varying the number of cells retrieved from one umbilical cord. The costs are expressed in USD (US dollars).

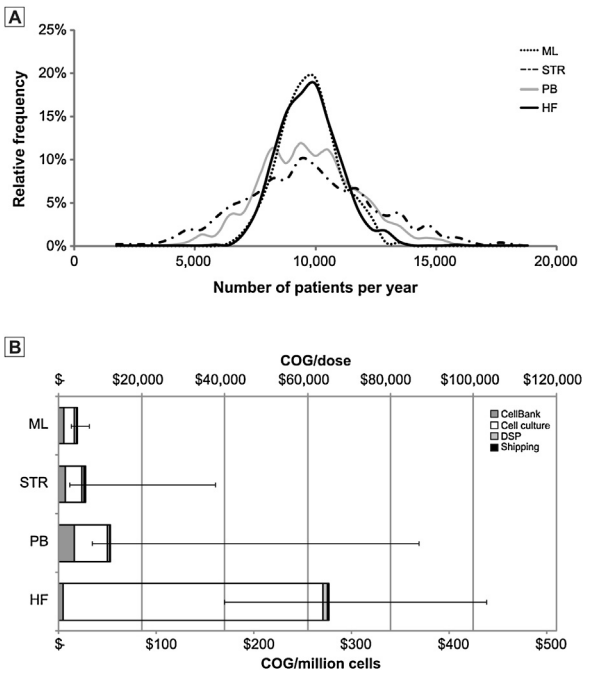

Fig. 4. **(A)** Distribution of number of doses produced per year using different technologies. The standard deviation for the different technologies were 666.3, 2,919, 31,278 and 8,347 for ML, STR PB and HF respectively. (**B)** COG breakdown per process stage with the error bars showing the min and max total COG/dose and COG/million cells across different technologies. The parameters used in this analysis were: the initial number of cells per cell bank, the technology specific doubling time and harvesting efficiency, the patient weight and the batch failure rate. The costs are expressed in USD (US dollars).

the cell bank costs follow the same trends as observed in Fig. 3A, with PB having the highest cell bank costs per dose that are up to 4 times the cost with ML due to difficulties in the harvesting process mentioned in Section 3.1.

3.3.2. *Throughput and cost effectiveness study*

Process robustness is highly important in any cell therapy process, not only because it affects the COG, but also because it can affect the ability to meet market demand [23].

Fig. 4A shows the variation in yearly throughput (number of doses per year) across the different technologies. This figure shows that all technologies have a mean value of 10,000 doses per year (desirable demand). However, when the data from the practical experiments (Table 3) is applied to the tool, variation in throughput occurs. Although all technologies have a 50% probability of achieving the desired demand, when using STR and PB, the high variability in cells harvesting efficiency causes a wide distribution in the yearly throughput with a 5% and 1% chance of achieving 5,000 doses per year (*i.e.* 50% of the desired demand) respectively. If a restriction was set such that the minimum tolerable annual throughput is 8,000 doses (i.e. 80% of the desired demand) the behavior of the technologies would cause a 5% probability of being below this target with HF and ML, 15% with PB and 20% with STR.

Fig. 4B shows the COG/dose and COG/million cells across the different technologies per process stage. It is clear that the ML is the most cost-effective and robust technology with a COG/dose of USD 4.5k followed by STR with a COG/dose of USD 6.5k. This can be attributed to the fact that although similar yields of cell number (cells/cm^2) were achieved with these technologies, the harvesting efficiency achieved with STR (60%) is significantly lower than the harvesting efficiency achieved with ML (100%) (Fig. 1). Previous studies have shown that if similar harvest densities were achieved for both technologies, STR would become more cost effective than ML [23]. In this case, if the harvest density of a process employing STRs was optimized to the level attained with ML, then the COG/dose of the STR route would fall to USD 3.7k, making the STR technology the most attractive option. STR has a high variability in COG/dose due to the large standard deviation in harvesting efficiency observed experimentally (Table 3). PBs are more robust than STRs as the standard deviation in harvesting efficiency is lower, however they have a higher mean COG/dose (USD 12.6k), mainly attributed to their low harvesting efficiency. In contrast, Pluristem Therapeutics Inc. has reported significant cost savings at 10,000 doses per year when switching to PB from ML, including a 40% reduction in culture media consumption [50]. In the present work, the media consumption was also significantly lower in PB when compared to ML (Table 1). The tool predicted that HF would have the highest mean COG/dose (USD 65.1k) due to the high bioreactor consumables costs per cm^2 (55 times more expensive than ML), the high equipment costs and the low harvesting density (9.800 cells/cm^2), and the limited capacity which increases the number of HF units required per lot. Moreover, even though the labour requirement for HF is lower than the labour requirement for ML (Table 1), the savings in labour costs are not high enough to make up for the higher equipment and consumable costs. Although HF has no standard deviation in harvesting efficiency, they have a relatively high standard deviation in the expansion fold of cells. The distributions generated appear to be skewed towards higher values of COG/dose, due to the fact that the COG/dose is given by the COG/year divided by the number of doses produced per year, with the latter being a distribution (Fig. 4A). The inverse of the number of doses per year causes the shift seen towards lower doses per year (*i.e.* higher COG/dose). This shift is more pronounced in technologies with higher variability in number of doses per year (STR and PB). Fig. 4B also shows that the process stage with the highest costs is the cell culture stage followed by the cell banking and DSP stages.

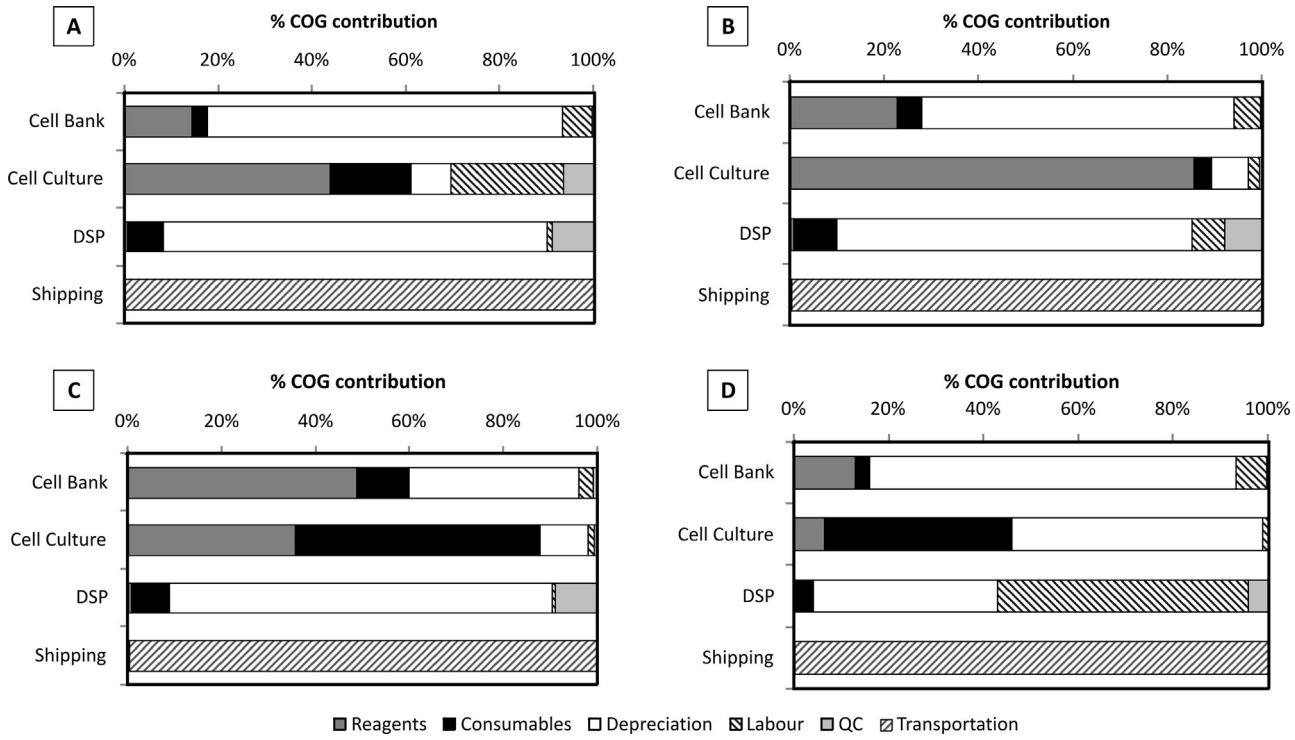

Fig. 5. Percentage contribution towards the COG/dose of the different cost categories across the different manufacturing stages for (**A**) ML, (**B**) STR, (**C**) PB and (**D**) HF.

3.3.3. *Key cost drivers*

In order to identify the key areas where additional development would result in an optimized process, it is important to first understand which parameters have the greatest impact on the COG and hence act as the key cost drivers.

Fig. 5 shows the different cost categories per process stage across different technologies. In the cell bank stage, most technologies follow the same trend, with the depreciation costs being the major cost driver, due to the fact that this step is carried out using 40-layer cell culture vessels, requiring automated manipulators costing USD 425k each. On the other hand, PB (Fig. 5C) follows a different pattern, demonstrating that the key cost drivers for this technology at the cell bank stage are the reagent costs, namely the culture media costs. The depreciation costs at the cell bank stage are the same across all the technologies, however, more MCBs are required when using PB (approx. 68 donors per year) and hence the amount of reagents and consumables required is greater increasing the burden of these components in the cell bank COG. A similar trend is observed in STR (Fig. 5B), as this technology requires 18 UC donors per year, which is more than ML and HF (10 and 9 respectively).

The cell culture process is the stage with the highest impact on COG across all technologies (Fig. 4B) and it is where technologies differ the most in cost drivers. For ML, the key cost drivers are reagents, consumables and labor. These cell culture flasks are not automated and hence, rely on manual operation therefore, labor cost have a bigger impact on COG than the depreciation costs. STRs (Fig. 5B) have the lowest consumables costs/cm^2 across all technologies (Table 1) and, given its high capacity, a single unit is used decreasing labor and equipment costs per million cells, and hence making culture media costs the key cost driver. Automation causes PB and HF (Fig. 5C and D) to follow the same trends in labor and equipment costs as STRs; both bioreactors have consumables as a key cost driver, PBs due to its low culture media consumption and HF due to the high costs per consumable cartridge.

In the DSP cost-breakdown of most technologies, the depreciation costs are the key cost driver, as fluidized bed centrifuges (kSep®, Sartorius, Göttingen, Germany) were used for cell wash and concentration. In HF, the trends are slightly different. This is explained by the fact that the model calculates the maximum number of operators required to carry out a HF-based process, and distributes the labor costs across stages according to the number of hours spent on each stage. Due to the high automation of the HF bioreactors, the number of hours spent in USP is low and similar to those in DSP; this even distribution of labor costs between USP and DSP causes for a higher proportion of these costs to be attributed to DSP in HF-based processes with respect to other technologies.

The shipping costs are composed of two categories: labor and transportation costs. Given the assumption that a team of 3 warehouse operators can process the shipping of 10,000 doses [33], the shipping labor costs per dose are relatively small and therefore, the transportation costs dominate the shipping costs.

3.3.4. *Reimbursement analysis*

Reimbursement strategies differ across countries and hence, a product which is commercially successful in one country may not be in others. Considering the reimbursement strategy in the chosen country for product commercialization will help set COG targets to achieve satisfactory gross margins.

Fig. 6 shows the percentage change in COG required for the COG to be 15% of sales across different technologies under two reimbursement regimes. Scenarios with no change correspond to situations where no improvement is required to meet this target. Negative scenarios show the percentage reduction in COG required for technologies to be competitive at that particular selling price.

The two reimbursement strategies selected were based on (a) the UK's National Institute of Health and Care Excellence (NICE) and (b) the allogeneic MSC-based treatment for GvHD by Mesoblast to be released in Japan – TEMCEL®. The selling price for these reimbursements strategies was USD 40k/dose (per quality adjusted life years-QALY) and USD 98/million cells (USD 7k per bag of 72 million cells) respectively [51–53]. The selling price for TEMCEL® was

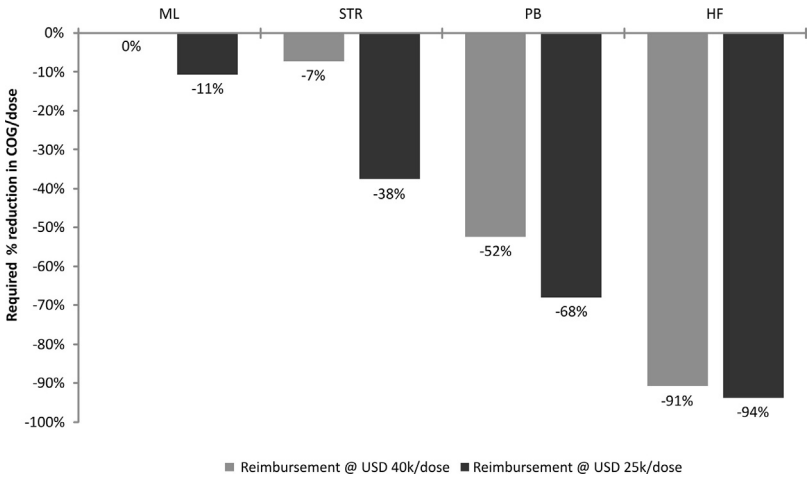

Fig. 6. Percentage increase/decrease in COG/dose required to achieve 85% gross margin across different technologies at the current NICE reimbursement and the reimbursement of two different MSC-based cell therapy products. The value of reimbursement is expressed in USD (US dollars).

adapted to the dose size used in this article (4×10^6 cells/kg and 68.6 kg) and was of the order of USD 25k/dose.

The results show that under reimbursement based on NICE recommendations (USD 40k/dose of UCM MSC), only ML would satisfy the target COG as% of sales set as the COG/dose of all other technologies is too high. Under the lower reimbursement levels extrapolated from TEMCEL® (USD 25k/dose of UCM MSC), no technology would satisfy the COG target. This does not mean that TEMCEL® is not commercially viable, and, although the dose size applied to patients using this therapy is higher than the dose sizes used in the clinical trial described in this study ($8 \times 2 \times 10^6$ cells/kg) [53], the manufacturing process of this product may be different to the ones described in this article. For example, if a higher market demand is targeted and higher lot sizes are used, then the COG/million cells would be lower as COG decreases with increasing scale [23]. Moreover, a better performance in cell doubling time and harvesting efficiency will result in a more cost-effective process. Furthermore, often catalogue prices for equipment and materials do not apply at larger scale processes as vendors can offer a bulk purchase discount, enhancing the reduction in COG with increasing demand; this factor is not accounted for in this article. Looking at the worst reimbursement case scenario (TEMCEL®) and at the key cost drivers of the different technologies (Fig. 5), it is possible to make recommendations for the current process to reach satisfactory COG as% of sales. In ML and STR the key cost driver is the culture media cost. Therefore, a 46% (USD 243/L) and a 69% (USD 139.5/L) reduction in the media cost (from bulk purchase discount or in-house culture media preparation) would result in satisfactory COG as% of sales for ML and STR respectively. The key cost drivers in PB are the consumables and culture media costs; one of the reasons for this is the low detachment efficiency of these bioreactors. Even though Fig. 6 shows that a COG reduction of 68% is required, drastic process changes are necessary in order to achieve this COG target. This combination of changes includes: increasing the harvest efficiency to 85%, decreasing the media costs by 77% (USD 103.5/L), reducing the bioreactor costs cost/cm^2 by 90% (USD 0.13×10^{-12}/cm^2) and the equipment costs by 90% (USD 30k/unit). HF key cost drivers are consumables and depreciation costs. This is due to a combination of factors: these bioreactors have the highest consumable costs/cm^2 as well as relatively high equipment costs for their capacity (Table 1). Moreover, the harvesting density achieved with this bioreactor (cells/cm^2) is relatively low (Table 3). In order for this bioreactor to be competitive with the other technologies under this reimbursement scenario, a dramatic increase in harvesting density is required (70,000 cells/cm^2), as well as a 85% reduction in consumable costs and equipment costs (to USD 0.09/cm^2 and USD 22.5k per unit respectively) and a 28% saving medium costs is also required (USD 234/L).

4. Conclusion

The experimental and economic evaluation of different culture technologies for the expansion of MSC is critical for commercial exploitation of MSC-based cell therapies. The results here presented show that the cell culture technology with the most promising experimental results in terms of expansion level, cell functionality and scalability may not be the optimal choice from a cost perspective. UCM MSC expanded in HF showed a higher proliferation rate, fold-increase and harvesting efficiency when compared to ML, STR and PB. However, HF was found to be the least cost-effective technology, presenting, high consumable costs/cm^2 and equipment costs and low harvesting density (reducing the capacity of this bioreactor). ML was found to be the most cost-effective and robust technology for the specific scenario evaluated. Results also revealed that the economic feasibility of the different technologies is greatly dependent on the reimbursement scenario selected, and there are industrially relevant manufacturing scenarios for which none of the technologies explored will result in satisfactory COG as% of sales. For example, for a product with a selling price of USD 25k/dose, reductions in media costs of 45–60% would be required in order to meet a COG as% sales target of 15% when using multilayer flasks and stirred tank bioreactors. For the remaining technologies, dramatic improvements in harvest density, harvesting efficiency as well as significant reductions in materials and consumable costs are required in order to reach the same COG target. This indicates that many studies are still needed to establish an optimized manufacturing process.

Acknowledgments

This work was financially supported by FAPESP (2012/23228-4; 2013/23599-5), CTC— Center for Cell-based Therapies (FAPESP 2013/08135-2) and National Institute of Science and Technology in Stem Cell and Cell Therapy (CNPq 573754-2008-0 and FAPESP 2008/578773). The authors also acknowledge Patricia Viana Bonini for flow cytometer technical assistance. Financial support for TDP Chilima from the UK Engineering and Physical Sciences Research Council (EPSRC) and Pall Life Sciences is gratefully acknowledged (Grant Code: EP/G034656/1). The Advanced Centre for Biochemical Engineering at UCL hosts the Future Targeted Healthcare Manufac-

turing Hub in collaboration with UK universities and with funding from the EPSRC and a consortium of industry and government users.

Appendix A. Supplementary data

Supplementary data associated with this article can be found, in the online version, at https://doi.org/10.1016/j.bej.2018.02.018.

References

[1] A. Trouson, R.G. Thakar, G. Lomax, D. Gibbons, Clinical trials for stem cell therapies, BMC Med. 9 (52) (2011) 1–7.
[2] F. dos Santos, P. Andrade, C.L. da Silva, J. Cabral, Bioreactor design for clinical-grade expansion of stem cells, Biotechnol. J. 8 (6) (2014) 644–654.
[3] P. Hanley, Z. Mei, A. Durett, M. da Graca Cabreira-Harrison, M. Klis, W. Li, Y. Zhao, B. Yang, K. Parsha, O. Mir, F. Vahidy, D. Bloom, R. Rice, P. Hematti, S. Savitz, A. Gee, Efficient manufacturing of therapeutic mesenchymal stromal cells with the use of the Quantum Cell Expansion System, Cytotherapy 16 (8) (2014) 1048–1058.
[4] D. Kehoe, A. Schnitzler, J. Simler, A. DiLeo, A. Ball, Scale-up of human mesenchymal stem cells on microcarriers in suspension in a single-use bioreactor, BioPharm. Int. 25 (3) (2012) 28–38.
[5] A. Mizukami, M. Orellana, S. Caruso, K. de Lima Prata, D.T. Covas, K. Swiech, Efficient expansion of mesenchymal stromal cells in a disposable fixed bed culture system, Biotechnol. Progress 29 (2) (2013) 568–572.
[6] Q. Rafiq, K. Brosnan, K. Coopman, A. Nienow, C. Hewitt, Culture of human mesenchymal stem cells on microcarriers in a 5L stirred-tank bioreactor, Biotechnol. Lett. 35 (8) (2013) 1233–1245.
[7] N. Timmins, M. Kiel, M. Gunther, C. Heazlewood, M. Doran, G. Brooke, K. Atkinson, Closed system isolation and scalable expansion of human placental mesenchymal stem cells, Biotechnol. Bioeng. 109 (7) (2012) 1817–1826.
[8] A.K. Chen, S. Reuveny, S.K. Oh, Application of human mesenchymal and pluripotent stem cell microcarrier cultures in cellular therapy: achievements and future direction, Biotechnol. Adv. 31 (7) (2013) 1032–1046.
[9] K.M. Panchalingam, S. Jung, L. Rosenberg, L.A. Behie, Bioprocessing strategies for the large-scale production of human mesenchymal stem cells: a review, Stem Cell Res. Ther. 6 (2015) 225.
[10] D. Jing, N. Sunil, P. Sandhya, A. Manjula, D. Kehoe, J. Murrel, M. Rook, K. Niss, Growth kinetics of human mesenchymal stem cells in a 3-L single-use, stirred-tank bioreactor, BioPharm. Int. 26 (4) (2013).
[11] A. Simaria, S. Hassan, H. Varadaraju, J. Rowley, K. Warren, P. Vanek, S.S. Farid, Allogeneic cell therapy bioprocess economics and optimization: single-use cell expansion technologies, Biotechnol. Bioeng. 111 (1) (2013) 69–83.
[12] M. Jones, M. Varella-Garcia, M. Skokan, S. Bryce, J. Schowinsky, R. Peters, B. Vang, M. Brecheisen, T. Startz, N. Frank, B. Nankervis, Genetic stability of bone marrow-derived human mesenchymal stromal cells in the Quantum System, Cytotherapy 15 (11) (2013) 1323–1339.
[13] P. Nold, C. Brendel, A. Neubauer, G. Bein, H. Hackstein, Good manufacturing practice-compliant animal-free expansion of human bone marrow derived mesenchymal stroma cells in a closed hollow-fiber-based bioreactor, Biochem. Biophys. Res. Commun. 430 (1) (2013) 325–330.
[14] C. Lechanteur, S. Baila, M.E. Janssen, O. Giet, A. Briquet, E. Baudoux, Y. Beguin, Large-scale clinical expansion of mesenchymal stem cells in the GMP-compliant closed automated Quantum® cell expansion system: comparison with expansion in traditional T-Flasks, J. Stem Cell Res. Ther. 4 (8) (2014) 1–11.
[15] M. Haack-Sorensen, B. Follin, M. Juhl, S.K. Brorsen, R.H. Sondergaard, J. Kastrup, A. Ekblond, Culture expansion of adipose derived stromal cells. A closed automated Quantum Cell Expansion System compared with manual flask-based culture, J. Transl. Med. 14 (1) (2016) 319.
[16] R. Allmendinger, A. Simaria, S.S. Farid, Multiobjective evolutionary optimization in antibody purification process design, Biochem. Eng. J. 91 (2014) 250–264.
[17] J. Pollock, G. Bolton, J. Coffman, S. Ho, D. Bracewell, S.S. Farid, Optimising the design and operation of semi-continuous affinity chromatography for clinical and commercial manufacture, J. Chromatogr. A 1284 (2013) 17–27.
[18] A. Stonier, A. Simaria, M. Smith, S.S. Farid, Decisional tool to assess current and future process robustness in an antibody purification facility, Biotechnol. Progr. 28 (4) (2012) 1019–1028.
[19] S. Hassan, A. Simaria, H. Varadaraju, S. Gupta, K. Warren, S.S. Farid, Allogeneic cell therapy bioprocess economics and optimization: downstream processing decisions, Regen. Med. 10 (5) (2015) 591–609.
[20] S. Hassan, H. Huang, K. Warren, B. Mahdavi, D. Smith, S. Jong, S.S. Farid, Process change evaluation framework for allogeneic cell therapies: impact on drug development and commercialization, Regen. Med. 11 (3) (2016) 287–305.
[21] M. Jenkins, J. Bilsland, T. Allsopp, S. Ho, S.S. Farid, Patient-specific hiPSC bioprocessing for drug screening: bioprocess economics and optimization, Biochem. Eng. J. 108 (2016) 84–97.
[22] T.D.P. Chilima, F. Moncaubeig, M. Egloff, T. Bovy, S.S. Farid, Impact of allogeneic stem cell manufacturing decisions on cost of goods, process robustness and reimbursement, Biochem. Eng. J. (2018) (under review for same special issue).
[23] T.D.P. Chilima, T. Bovy, S.S. Farid, Designing the optimal manufacturing strategy for an adherent allogeneic cell therapy, Bioprocess Int. 14 (9) (2016) 24–32.
[24] S. Colowick, N. Kaplan, Methods in Enzymology, Academic Press, New York, 1964.
[25] M. Hayat, Stem Cells and Cancer Stem Cells, Springer Netherlands, Netherland, 2012, pp. 319.
[26] J. Reiser, X. Zhang, C. Hemenway, D. Mondal, L. Pradhan, V. La Russa, Potential of mesenchymal stem cells in gene therapy approaches for inherited and acquired diseases, Expert Opin. Biol. Ther. 5 (12) (2005) 1571–1584.
[27] Q. Zhao, C. Gregory, R. Lee, R. Reger, L. Qin, B. Hai, M. Park, N. Yoon, B. Clough, E. McNeill, D. Prockop, F. Liu, MSCs derived from iPSCs with a modified protocol are tumor-tropic but have much less potential to promote tumors than bone marrow MSCs, Proc. Natl. Acad. Sci. 112 (2) (2014) 530–535.
[28] K.L. Prata, G.C. de Santis, M.D. Orellana, P.V. Palma, M.S. Brassesco, D.T. Covas, Cryopreservation of umbilical cord mesenchymal cells in xenofree conditions, Cytotherapy 14 (2012) 694–700.
[29] GlobeNewswire News Room, Mesoblastâ€™s Japan Licensee Receives Pricing for TEMCELLÂ® HS Inj. for Treatment of Acute Graft Versus Host Disease, 2018, http://globenewswire.com/news-release/2015/11/27/790909/0/en/Mesoblast-s-Japan-Licensee-Receives-Pricing-for-TEMCELL-HS-Inj-for-Treatment-of-Acute-Graft-Versus-Host-Disease.html. (Accessed: 15 February 2018).
[30] M. Barton-Burke, D. Dwinell, L. Kafkas, C. Lavalley, H. Sands, C. Proctor, E. Johnson, Graft-versus-host disease: a complex long-term side effect of hematopoietic stem cell transplant, Oncology 22 (11) (2008) 31–45.
[31] J. Wingard, S. Piantadosi, G. Vogelsang, E. Farmer, D. Jabs, L. Levin, W. Beschorner, R. Cahill, D. Miller, D. Harrison, Predictors of death from chronic graft-versus-host disease after bone marrow transplantation, Blood 74 (4) (1989) 1428–1435.
[32] S. Walpole, D. Prieto-Merino, P. Edwards, J. Cleland, G. Stevens, I. Roberts, The weight of nations: an estimation of adult human biomass, BMC Public Health 12 (1) (2012) 439.
[33] M. Lowdell, Phase I and II Manufacturing, in UCL- Cell Therapy Catapult MBI Cell Therapy, 2014 (London).
[34] J. Rowley, E. Abraham, H. Brandwein, S. Oh, Meeting lot-size challenges of manufacturing adherent cells for therapy, Bioprocess Int. 10 (2012) 16–22.
[35] D. Schop, F.W. Janssen, L.D. van Rijn, H. Fernandes, R.M. Bloem, J.D. de Bruijn, R. van Dijkhuizen-Radersma, Growth, metabolism, and growth inhibitors of mesenchymal stem cells, Tissue Eng. Part A 15 (2009) 2653–2663.
[36] A.W. Nienow, Q.A. Rafiq, K. Coopman, C.J. Hewitt, A potentially scalable method for the harvesting of hMSCs from microcarriers, Biochem. Eng. J. 85 (2014) 79–88.
[37] G. Eibes, F. dos Santos, P.Z. Andrade, J.S. Boura, M.M. Abecasis, C.L. da Silva, J.M. Cabral, Maximizing the ex vivo expansion of human mesenchymal stem cells using a microcarrier-based stirred culture system, J. Biotechnol. 146 (4) (2010) 194–197.
[38] C. Ferrari, F. Balandras, E. Guedon, E. Olmos, I. Chevalot, A. Marc, Limiting cell aggregation during mesenchymal stem cell expansion on microcarriers, Biotechnol. Progr. 28 (3) (2012) 780–787.
[39] S.R. Caruso, M.D. Orellana, A. Mizukami, T.R. Fernandes, A.M. Fontes, C.A. Suazo, V.C. Oliveira, D.T. Covas, K. Swiech, Growth and functional harvesting of human mesenchymal stromal cells cultured on a microcarrier-based system, Biotechnol. Progr. 30 (4) (2014) 889–895.
[40] A. Mizukami, A. Fernandes-Platzgummer, J.G. Carmelo, K. Swiech, D.T. Covas, J.M.S. Cabral, C.L. da Silva, Stirred tank bioreactor culture combined with serum-/xenogeneic-free culture medium enables an efficient expansion of umbilical cord-derived mesenchymal stem/stromal cells, Biotechnol. J. 11 (2016) 1048–1059.
[41] T.K.-P. Goh, Z.-Y. Zhang, A.K.-L. Chen, S. Reuveny, M. Choolani, J.K.Y. Chan, S.K.-W. Oh, Microcarrier culture for efficient expansion and osteogenic differentiation of human fetal mesenchymal stem cells, BioRes. Open Access 2 (2) (2013) 84–97.
[43] D. Wang, W. Liu, B. Han, R. Xu, The bioreactor: a powerful tool for large-scale culture of animal cells, Curr. Pharm. Biotechnol. 6 (5) (2005) 397–403.
[44] J. Hupfeld, I.H. Gorr, C. Schwald, N. Beaucamp, K. Wiechmann, K. Kuentzer, R. Huss, B. Rieger, M. Neubauer, H. Wegmeyer, Modulation of mesenchymal stromal cell characteristics by microcarrier culture in bioreactors, Biotechnol. Bioeng. 111 (11) (2014) 2290–2302.
[45] C. Schirmaier, V. Jossen, S.C. Kaiser, F. Jüngerkes, S. Brill, A. Safavi-Nab, A. Siehoff, C. van den Bos, D. Eibl, R. Eibl, Scale-up of adipose tissue-derived mesenchymal stem cell production in stirred single-use bioreactors under low-serum conditions, Eng. Life Sci. 14 (2014) 292–303.
[46] M. Dominici, K. Le Blanc, I. Mueller, I. Slaper-Cortenbach, F. Marini, D. Krause, R. Deans, A. Keating, Dj. Prockop, E. Horwitz, Minimal criteria for defining multipotent mesenchymal stromal cells. The International Society for Cellular Therapy position statement, Cytotherapy 4 (2006) 315–317.
[47] J.G. Carmelo, A.M. Fernandes-Platzgummer, M.M. Diogo, C.L. da Silva, J.M. Cabral, A xeno-free microcarrier-based stirred culture system for the scalable expansion of human mesenchymal stem/stromal cells isolated from bone marrow and adipose tissue, Biotechnol. J. 10 (2015) 1235–1247.
[48] M. Mendicino, A.M. Bailey, K. Wonnacott, R.K. Puri, S.R. Bauer, MSC-based product characterization for clinical trials: an FDA perspective, Cell Stem Cell 14 (2) (2014) 141–145.

[49] M.L. Torre, E. Lucarelli, S. Guidi, M. Ferrari, G. Alessandri, L. De Girolamo, A. Pessina, I. Ferrero, Ex vivo expanded mesenchymal stromal cell minimal quality requirements for clinical application, Stem Cells Dev. 15 (6) (2015) 677–685.
[50] O. Karnieli, B. Gur-Lavie, Cell therapy: early process development and optimization of the manufacturing process are critical to ensure viability of the product, quality, consistency and cost efficiency, J. Commer. Biotechnol. 21 (1) (2015).
[51] Carrying NICE over the Threshold, Blog News NICE, 2018, https://www.nice.org.uk/news/blog/carrying-nice-over-the-threshold. (Accessed 15 February 2018).
[52] GlobeNewswire News Room, Mesoblast Provides Update on Clinical Programs of Prochymal for Crohn's Disease and Acute Graft Versus Host Disease, 2014, http://globenewswire.com/news-release/2014/04/29/630744/10078747/en/Mesoblast-Provides-Update-on-Clinical-Programs-of-Prochymal-for-Crohn-s-Disease-and-Acute-Graft-Versus-Host-Disease.html. (Accessed 08 February 2016).
[53] Acesurgical, Osteocel Plus, 2018, http://www.acesurgical.com/index.php/downloads/dl/file/id/8/info_ace_osteocel.pdf. (Accessed 15 February 2018).